Nanotechnology Perceptions
ISSN 1660-6795
www.nano-*ntp.com*

Comparative Magnetic Study Of Nanosized Substitutional Nickel Spinel Ferrite

R.M.Meshram[1], P.N.Ukey[2],D.S.Choudhary[3], Y.S.Bopche[4], P.A.Katre[5], K.Pushpanjali Patra[6]

[1]M.B.Patel College,Sakoli, [2]S.S.Jaiswal College, Arjuni/Mor,[3]D.B.Science College, Gondia, [4]D.B.Science College, Gondia,[5]M.B.Patel College,Sakoli,[6]Ramdeobaba Univerrsity, Nagpur

The single phased polycrystalline samples of inverse spinel $Ni_{0.5}(Mg_{0.5-x}Zn_x)Fe_2O_4$ (x = 0.0 to 0.5), have been prepared using sol-gel technique and reported its magnetic and structural properties. Structural analysis reveals the series is crystallizes into cubic structure in $Fd\bar{3}m$ space group. The increase in Zn concentration correlates with an elevation in lattice characteristics, including unit cell volume. An increase in the average crystalize size has been obtained and a drop in the micro strain parameter. M-H loops measured at 300 K show a typical ferrimagnetic loop with a clear saturation. At 300 K, (M-H) loops demonstrated increase in coercivity (H_C) and retentivity (M_r)value after Zn substitution. However, the observed saturation magnetization (M_S) shows some abnormal change attributed to the movement of some of the Zn ion to the tetrahedral site.

Introduction:

There are ferrimagnetic materials belong to the ferrite family and there are three kinds of ferrites such as spinel, garnet and hexaferrite. These ferrites can be distinguishing on the basis of their crystal structure. Spinel Compounds are one of the important groups of magnetic oxides with mostly cubic crystal structure. Spinel oxide compounds represented their general chemical formula as AB_2O_4, Where A and B are divalent and trivalent cations respectively and O is an anion (Oxygen). The cubic crystal shape with space group is the most common for spinel compounds during crystallization $Fd\bar{3}m$ [1, 2]. Spinel structure is a close packed face-centered cubic lattice formed by oxygen anions. Spinels are divided into three categories viz. normal spinels, inverse spinels and mixed spinels, based on the distribution of A and B ionsin the available two sublattices,. In normal spinels, A and B ions occupy the tetrahedral and octahedral sites respectively.$NiCr_2O_4$, $CoCr_2O_4$, and $MnCr_2O_4$ are some examples of normal spinel [3]. Conversely, in inverse spinels, half of the B ions occupy the tetrahedral sites whereas A ions along with the other half of B ions occupy the octahedral sites. $NiFe_2O_4$, Fe_3O_4, $MgGa_2O_4$ are some of the examples of inverse spinel. [4]. Mixed spinel can be produced when A and B cations randomly occupy the tetrahedral or octahedral positions in most spinels, depending on the synthesis conditions [4,5]. In normal spinel the unit cell consists of 8 units of AB_2O_4, i.e. 24 cations (8 A-type & 16 B-type) and 32 anions. Eight of the 24 cations are

dispersed among the 64 tetrahedral sites that are available, while the remaining 16 are dispersed among the 32 octahedral sites. Spinel compounds in general crystallize in to cubic structure with space group $Fd\bar{3}m$.However, some spinels for example $NiCr_2O_4$ crystallize in tetragonal structure with space group $I4_1/amd$ below certain temperature where John Teller distortion takes place [6].

Spinel ferrites with chemical formula AFe_2O_4 are important group of materials because of their enhanced electrical, magnetic, and optical properties. With a high value of saturation magnetization, they are technologically important for variety of applications. They have been thoroughly examined in the recent years for application in the information storage device, magnetic bulk cores, magnetic fluids, microwave absorbers, electrode in energy storage device, as catalysts and high frequency devices [7 – 11]. Its unit cell has 32 oxygen atoms in a cubic closed packing with 8 tetrahedral and 16 octahedral occupied sites, just like spinel chromite. By substituting divalent cations in A^{2+} sites, it is possible to obtain significant deviations in physical, electrical and magnetic properties of these ferrites.

$NiFe_2O_4$ is one of the soft ferrite magnetic material with cubic crystal structure. Unlike nickel chromite it has inverse spinel structure, where Ni^{2+} ion occupies the octahedral sites andhence Jahn-teller inactive. The spinel ferrite shows interesting properties like exchange bias and memory effect [12, 13]. This ferrite's high permeability and low electrical conductivity make it ideal for use in switch mode power supply, transformer cores, and inductors [14]. Influence of A^{2+} ions on Gas sensing properties of this compound has been investigated at different temperatures [15]. Magnetocaloric effect is another important phenomenon shown by nickel ferrite [16, 17] and it has technological applications for energy efficient, environment friendly magnetic refrigeration. Due to low eddy current, dielectric loss, coercivities and good chemical stability [18, 19] these materials are one of the natural choices for application. Nickel ferrites are considered as one of the most versatile compounds among ferrites. Using room-temperature neutron diffraction measurements, Hastings et al. (1953) first reported the chemical and magnetic characteristics of NiFe2O4 [20]. However, owing to its new applications in areas that encompass magnetic recording media [21, 22], spintronics and actuators [23], magnetic memories [24, 25], microwave devices [26, 27], catalysts [28, 29], magnetic sensors [30], and biotechnology [31, 32], this material receives more attention from scientists and researchers after the 19th century etc. The anti-parallel alignment of the magnetic moments of the Fe3+ ions at the tetrahedral (A) sites and the Ni2+ and Fe3+ ions at the octahedral (B) sites causes the spinel ferrite to display ferrimagnetism (FIM). The material can exhibit several interesting properties based on the synthesis process. In this work, the preparation of$Ni_{0.5}(Mg_{0.5-x}Zn_x)Fe_2O_4$ (x = 0.0 to 0.5) Sol-gel compounds and their structural and magnetic characteristics have been reviewed and compared with a constant magnesium content.

Experimental:

Single phase polycrystalline samples of $Ni_{0.5}(Mg_{0.5-x}Zn_x)Fe_2O_4$ (x = 0.0 to 0.5) were synthesized by sol-gel technique. An appropriate amount of nickel nitrate (Ni(NO3)2_6H2O) (99.9%, Merck), zinc nitrate (Zn(NO3)2_4H2O) (99.9%, Merck), iron nitrate

(Fe(NO3)3_9H2O) (99.9%, Merck), and magnesium nitrate (Mg(NO3)2_6H2O) (99.9%, Merck) were dissolved in distilled water. Urea is mixed as fuel for autocumbustion. At room temperature, distilled water was used to dissolve the stoichiometer-sized amounts of precursors.

The resultant solution was agitated on a hot plate magnetic stirrer at 80°C until H_2O was evaporated and transformed into a brownish viscous gel. After self-cumbustion fine powder is formed. The calcinations were carried out at 800 °C for 6 hours.

Characterization:

To determine the crystal structure and phase purity of the compounds, powder X-ray diffraction (XRD) patterns were obtained at room temperature using a Rigaku TTRAX-III X-ray diffractometer with CuKα radiation (λ = 1.5406 Å). A Lake Shore make Vibrating Sample Magnetometer (VSM) has been used to record the magnetic data.

Result and Discussion:

1 XRD Analysis:

Powder X-ray diffraction patterns of all the samples of the series $Ni_{0.5}(Mg_{0.5-x}Zn_x)Fe_2O_4$is recorded at room temperature and is depicted in Figure.1. (a). The $Ni_{0.5}(Mg_{0.5-x}Zn_x)Fe_2O_4$ samples are observed in single phase form as per the powder X-ray diffraction (XRD) patterns recorded at room temperature. Here we have taken the data in the range of 25 to 75 degree with a step size of 0.02 degree. We were able to index the XRD peaks using the (h k l) planes to a single-phasecubic structure with space group $Fd\bar{3}m$ as shown in Figure.1. (a). The enlarged view of the most intense peak of (311) reflection in the range of $32 < 2\theta < 43°$ is found to shift towards higher 2θ (Bragg angle) with an rise in Zn concentration as shown in Figure.1. (b). This characteristic indicates a decline in the size of the particles or crystallites as well as the lattice characteristics. All the lattice parameters are tabulated in Table -1.

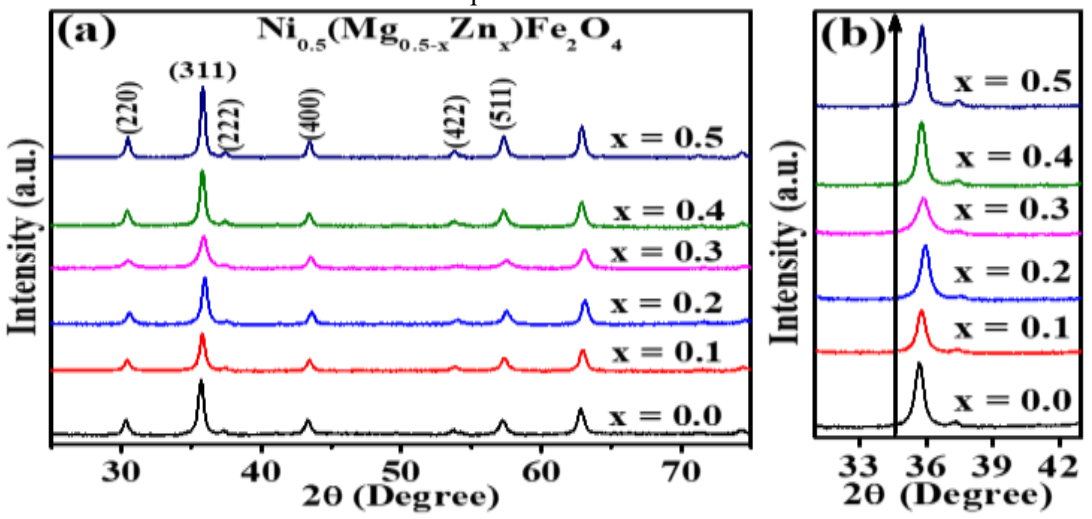

Figure.1. (a) Room temperature XRD patterns of $Ni_{0.5}(Mg_{0.5-x}Zn_x)Fe_2O_4$ (x = 0.0 - 0.5), and (b) enlarged view of (311) reflection at around $2\theta = 32^0$ to 43^0.

Table.1. Extracted structural parameters for the $Ni_{0.5}(Mg_{0.5-x}Zn_x)Fe_2O_4$series.

Sample	x = 0.0	x = 0.1	x = 0.2	x = 0.3	x = 0.4	x = 0.5
a (= b = c) (Å)	8.388	8.381	8.382	8.367	8.399	8.403
V (Å^3)	590.223	588.604	588.932	585.790	592.517	593.334
R_p	28.1	33.7	29.0	33.3	26.4	26.0
R_{wp}	13.7	15.3	13.9	18.5	12.2	12.5
R_{exp}	11.40	13.90	12.42	15.18	11.34	10.0
R_{Bragg}	1.55	3.08	0.911	1.72	1.12	1.17
R_f	1.64	6.01	0.953	1.23	1.60	1.08
χ^2(%)	1.44	1.21	1.26	1.48	1.15	1.57
Bond lengths (Å)						
d_{A-O}	3.4616	3.4677	3.4714	3.475	3.4779	3.4802
d_{B-O}	2.130	2.1283	2.1208	2.1171	2.1059	2.0838
d_{A-B}	3.4689	3.4744	3.4750	3.4776	3.4821	3.4837

Magnetic properties

To understand the magnetic behavior, the magnetic hysteresis (M-H) loops of all the samples have been recorded at 300 K (room temperature)at an applied field up to ±15 kOe as shown in Figure.5. (a).They all exhibit a visible hysteresis loop and the magnetization easily attains saturation at higher applied field, representing a typical ferrimagnetic (FIM) behaviour. In addition, with increasing external field, the dc magnetization increases monotonously and reaches to a saturation value from a field of 5 kOe applied field for all the loops. The enlarged view of the loop near coercivity is shown in Figure.5. (b). Its relatively low coercive field value suggests that all of the samples exhibit soft FIM behavior. All the magnetic parameters are tabulated in Table-2. The value of coercivity (H_c) and retentivity (M_r) is found to be increasing with Zn concentration indicating a increase in the anisotropy due to the Zn doping in the samples.

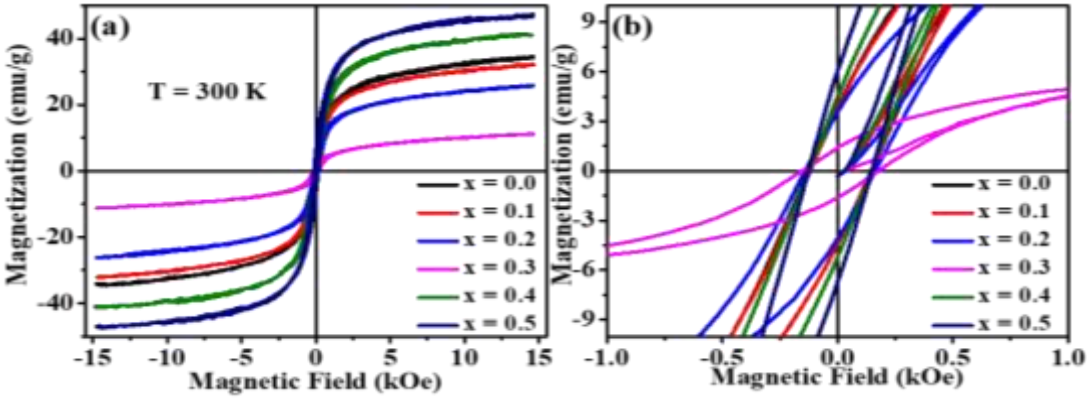

Figure.5. (a) M-H loops at 300 K, and (b) the expanded view of loops near coercive field for $Ni_{0.5}(Mg_{0.5-x}Zn_x)Fe_2O_4$ (x = 0.0 - 0.5)series.

Table-2. Estimated magnetic parameters of $Ni_{0.5}(Mg_{0.5-x}Zn_x)Fe_2O_4$ (x = 0.0 - 0.5) obtained from room temperature magnetic hysteresis loops.

Sample	**x = 0.0**	**x = 0.1**	**x = 0.2**	**x = 0.3**	**x = 0.4**	**x = 0.5**
H_C (Oe)	137	133	153	166	136	138
M_r (emu/g)	4.13	4.08	3.82	4.51	4.85	6.38
M_S (emu/g)	34.62	32.21	26.07	11.25	41.37	47.42

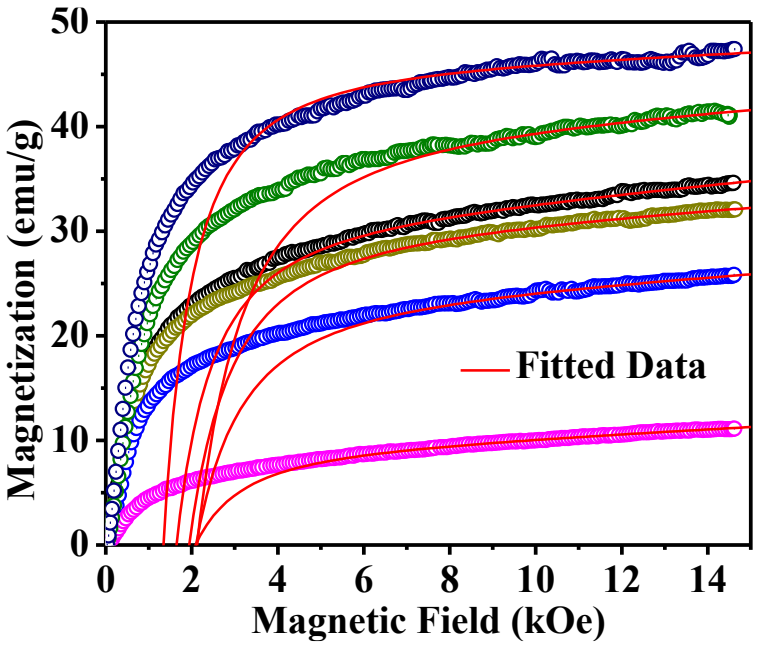

Figure.6. Initial M-H loop along with fitted data to LAS modelfor $Ni_{0.5}(Mg_{0.5-x}Zn_x)Fe_2O_4$ (x = 0.0 - 0.5)series.

To determine the magnetic parameters from the M-H loops and the magnetic saturation (MS) values of each sample, we have examined the initial M-H curves using the law of approach to saturation (LAS) model, as shown below [34],

$$M = M_S \left(1 - \frac{8K_1^2}{105\mu_0^2 M_S^2 H^2}\right) + bH \quad (2)$$

Here K_1represent a constant related to magneto-crystalline anisotropy and b is a constant related to forced magnetization at high field. The fitted initial loops to the LAS model are

displayed in the Figure.6. It can be observed that, the obtained data are well fitted to the LAS model. The obtained values of magnetic saturation (M_S) for all the samples are tabulated in the Table-2. It has been observed that the experimental values of M_S obtained for x = 0.0 is comparable with the previous report. Here, we have seen a decrease in the saturation (MS) value with Zn concentration up to x = 0.3, which indicates that the ion with the higher magnetic moment has partially been replaced by the ion with the lower magnetic moment. Which confirms the replacement of Mg with Zn, as Zn is a nonmagnetic ion it leads to a drop in the M_S value. However, at higher concentrated samples such as for x= 0.4 and 0.5 we have observed a rise in the M_S value which could be due to the transfer of few Zn ion towards the tetrahedral site.

The M-H curves for NixMg0.5Zn0.5-xFe2O4 (with x changing from 0.0, 0,1, 0.2, 0.3, 0.4, 0.5) samples at room temperature, on the other hand, reveal that Ni2+-doped samples transition from superparamagnetic to soft ferrimagnetic activity. Furthermore, it has been observed that the presence of diamagnetic Mg^{2+} and Zn^{2+} ions, which lack electron spin and do not contribute to magneto-crystalline anisotropy, induces the formation of superparamagnetic material [35].

The substitution of diamagnetic Zn^{2+} with magnetic Ni^{2+} introduces ferromagnetic characteristics. Ni2+ ions enhance magneto-crystalline anisotropy, allowing ferrites to maintain magnetic order and exhibit soft ferrimagnetic behavior [36].

With constant value of Ni^{2+} , the coerivity (Hc) decreses linearly with Zn^{2+} concentration, and saturation manetization (Ms) increses for lower concentration of Zn^{2+}, also reduce for higher concentration [37].

The squareness ratio and coercivity values confirm the superparamagnetic behaviour of NiMgZn nano-sized ferrites. The discrepancies in coercivity values may be due to significant LS coupling and super-exchange interactions between metal cations at tetrahedral and octahedral locations [38].

Magnetic study of $Mg_{0.5}Zn_{0.5-x}Ni_xFe_2O_4$reveals a transition from super paramagnetic behavior to soft ferrimagnetic nature with Ni^{2+} addition. Ferrite nanoparticles have demonstrated a decrease in saturation magnetization and an increase in coercivity with a reduction in crystallite size. It has been noted that the remanence ratio increases with Ni^{2+} concentration [39, 40].

In the magnetic study of $Ni_{0.5-x}Zn_{0.5}Mg_xFe_2O_4$ ferrites it is observed that the magnetic moment measurement reveal that the saturation magnetization (Ms) increases and coercivity(H) decreases with the increases in concentration of Mg^{2+} ions. Ms and Hc also show dependence on the annealing temperature.

When magnesium ions are used in place of nickel ions, the saturation magnetization value rises and the magnetization for the initial concentration decreases. Using Neel's two-sub lattice model, the redistribution of cations across accessible sites was used to explain the change in saturation magnetization values. When magnesium ions are added in excess, the magnetic moment of sites A and B is diluted, lowering the net magnetization value [41].

Conclusion:

We have successfully prepared the single phased polycrystalline samples of inverse spinel $Ni_{0.5}(Mg_{0.5-x}Zn_x)Fe_2O_4$ (x = 0.0 - 0.5), using sol-gel technique. Structural analysis reveals the series is formed under cubic structure in Fd-3m space group. With Zn doping we have

observed a rise in the lattice parameters as well as unit cell volume which confirms the replacement of Mg having lower ionic radius with that of Zn having higher ionic radius. An increase in the average crystallize size has been obtained and it lead to a drop in the micro strain parameter value. Revealing the decrease in the surface to volume ratio with Zn doping. M-H loops measured at 300 K show a typical ferrimagnetic loop with a clear saturation. Whereas, the smaller coercivity reveal a soft ferrimagnetic material. Coming to the saturation value it shows some abnormal change attributed to the movement of some of the Zn ion to the tetrahedral site.

$Mg_{0.5}Zn_{0.5-x}Ni_xFe_2O_4$ reveals a transition from super paramagnetic behavior to soft ferrimagnetic nature with Ni^{2+} addition.

In $Ni_{0.5-x}Zn_{0.5}Mg_xFe_2O_4$ the variation of Mg^{2+} and Ni^{2+} in Zn ferrites reduce the net magnetization.

References:

[1] K. E. Sickafus, J. M. Wills, N. W. Grimes, J. Am. Ceram. Soc. 82, (1999), 3279.
[2] R. W. Grimes, A. B. Anderson, A. H. Heuer, J. Am. Ceram. Soc. 111, (1989), 1.
[3] C. M. Brent, E. D. Jennifer, S. Ram, E. M. Stoudenmire, P. R. Arthur, J. Phys.: Condens. Matter 21 (2009) 216007.
[4] G. A. Sawatzky, F. Van Der Wounde, A. H. Morrish, Phys. Rev. 187 (1969) 747.
[5] V.W. J. Verhoeven, F. M. Mulder, and I. M. De Schepper, Phys. B (Amsterdam, Neth.) 276–278, (2000)950.
[6] V. Kocsis, S. Bordács, D. Varjas, K. Penc, A. Abouelsayed, C. A.Kuntscher, K. Ohgushi,Y. Tokura, and I.Kézsmárki, Phys. Rev. B 87, (2013)064416.
[7] V. Korenivski, R. B. van Dover, Y. Suzuki, E. M. Gyorgy, J. M. Philips, R. J. Felder, J. Appl. Phys. 79 (1996)5926.
[8] C. W. Nan, M. I. Bichurin, S. Dong, D. Viehland, G. Srinivasan, J. Appl. Phys. 103, (2008)031101.
[9] R. Y. Zheng, J. Wang, S. Ramakrishna, J. Appl. Phys. 104 (2008)034106.
[10] T. Mathew, B. B. Tope, N. R. Shiju, S. G. Hegde, B. S. Rao and C. S. Gopinath, Phys. Chem. Chem. Phys.,4, (2002)4260.
[11] K. Lazar, T. Mathew, Z. Koppany, J. Megyeri, V. Samuel, S. P. Mirajkar, B. S. Rao and L. Guczi, Phys. Chem. Chem. Phys.,4, (2002)3530.
[12] K. Nadeem, H. Krenn, J. Supercond Nov. Mag., 24, (2011)717.
[13] X. Zhao, S. Xu, L. Wang, X. Duan, and F. Zhang, Nano Res., 3, (2010)200.
[14] J.B. da Silva, N.D.S. Mohallem, J. Mag. Mag. Mater., 226, (2001)1393.
[15] A. Sutka, G. Mezinskisa, A. Lusis, M. Stingaciu, Sensors and Actuators B 171–172, (2012)354–360.
[16] S. Akhter, D. P. Paul, S. M. Hoque, M. A. Hakim, M. Hudl, R. Mathieu, P. Nordblad, J. Mag. Mag. Mater., 367, (2014)75.
[17] M.S. Anwar, Faheem Ahmed, Bon Heun Koo, ActaMaterialia 71, (2014)100.
[18] K. Verma, A. Kumar, D. Varshney, Current Applied Physics, 13, (2013)467-473.
[19] N. Ponpandian P. Balaya, A. Narayanasamy, J. PhysCondens. Matter 14, (2002)3221.

[20] J.M. Hastings, L.M. Corliss, Rev. Modern Phys. 25, (1953), 114.
[21] D.S. Jung, Y.C. Kang, J. Magn. Magn.Mater.321, (2009), 619.
[22] S.T. Hussain, S.R. Gilani, S.D. Ali, H.S. Bhatti, J. Alloy.Compd. 544, (2012), 99.
[23] A.D. Mani, I. Soibam, Physica B 507, (2017), 21.
[24] M.H. Dhaou, S. Hcini, A. Mallah, M.L. Bouazizi, A. Jemni, Appl. Phys. A 123, (2017), 8.
[25] P. Chavan, L.R. Naik, P.B. Belavi, G. Chavan, C.K. Ramesha, R.K. Kotnala, J. Electron Mater. 46, (2017), 188.
[26] D. Vladikova, L. Ilkov, S. Karbanov, Phys. Status Solidi A 121, (1990), 249.
[27] M. N. Ashiq, M.J. Iqbal, I.H. Gul, J. Alloys Compd. 487, (2009), 341.
[28] C.G. Ramankutty, S. Sugunan, Appl. Catal. A General 218, (2001), 39.
[29] J. Rawat, S. Rana, R.S. Srivastava, R.D.K. Misra, Mater. Sci. Eng. C 27, (2007), 540.
[30] Z. Jia, R.D.K. Misra, Mater. Technol. 26, (2011), 191.
[31] X. Wu, W. Chen, W. Wu, H. Li, C. Lin, J. Electron. Mater.46, (2017), 199.
[32] M. Rahimia, M. Eshraghi, P. Kameli, Ceram. Int. 40, (2014), 15569.
[34] S. Chakrabarty, A. Dutta, M. Pal, J. Alloys and Comp.625, (2015) 216.
[35] Lodhi, M.Yousaf, K. Mahmood, A. Mahmood, H. Malik, M.FarooqWarsi, I Shakir, M. Asghar, M. Khan. Current Applied Physics 14, no. 5 (2014): 716-720.
[36] Nikumbh, A. K., R. A. Pawar, D. V. Nighot, G. S. Gugale, M. D. Sangale, M. B. Khanvilkar, A. V. Nagawade. Journal of Magnetism and Magnetic Materials 355 (2014): 201-209.
[37] Tiwari, P., R. Verma, S. N. Kane, TetianaTatarchuk, F. Mazaleyrat. Materials Chemistry and Physics 229 (2019): 78-86.
[38] Akhtar, MajidNiaz, A. Rahman, A. B. Sulong, Muhammad Azhar Khan. Ceramics International 43, no. 5 (2017): 4357-4365.
[39]Sharma, Rohit, Prashant Thakur, Pankaj Sharma, and Vineet Sharma. Journal of Alloys and Compounds 704 (2017): 7-17.
[40] Satalkar, M., S. N. Kane, A. Ghosh, NandkishorGhodke, G. Barrera, F. Celegato, Marco Coisson, P. A. O. L. A. Tiberto, and Franco Vinai , ournal of alloys and compounds 615 (2014): S313-S316.
[41] Kavitha, N., and P. Manohar. "Magnetic and electrical properties of magnesium-substituted Ni–Zn ferrites." Journal of Superconductivity and Novel Magnetism 29 (2016): 2151-2157.